Lunar Surface Solar Origins Explorer (LunaSSOX)

Heliophysical Investigation of Mass Flow from the Sun to the Moon
Heliophysics of the Moon and from the Moon

John F. Cooper, Richard E. Hartle, Edward C. Sittler Jr
NASA Goddard Space Flight Center, Greenbelt, Maryland

Thanks to Joe Davila / NASA GSFC, Joe Minow / NASA MSFC, Richard Elphic / NASA ARC

Tom Seaver
NY Mets #41

Lunar Yogism: "It's like déjà vu all over again"

Yogi Berra
NY Yankees #8

LunaSSOX Mission Science Objectives

- **Measure, and enable predictive modeling of, plasma ion inputs to lunar surface volatile composition via orbital measurements**

  Upstream solar wind flow from Sun to lunar orbital environment

  Terrestrial contributions via ionospheric and magnetospheric flows

- **Map global distribution of volatile and refractory surface composition via imaging & pickup ions from ion sputtering**

  Distinguish regions dominated by external vs. any intrinsic sources

  Determine effects of crustal magnetic fields on surface composition

- **Remotely explore composition and dynamics of dust-plasma interaction components in solar F-corona region**

  Inner radial limits, composition, & sources of near-solar dust cloud

  Impact on “inner source” pickup ion composition for flow to Moon

LunaSSOX Relevance to NASA Strategic Goals

Strategic Sub-goal 3C: Advance scientific knowledge of the origin and history of the solar system, the potential for life elsewhere, and the hazards and resources present as humans explore space.

The solar wind plasma and energetic ion interaction with the Moon determines the global distribution of volatiles within the human-accessible regolith layer and ion sputtering can be utilized for resource mapping of the total volatile and refractory inventories. Full global 3-D hybrid code simulations will map global surface exposure to hazardous solar particle events.

Strategic Sub-Goal 3B: Understand the Sun and its effects on Earth and the solar system.

The Moon's remotely sensible surface and surface-accessible regolith records in its chemical composition the history of 4.5 billion years of solar wind and cosmic rays effects on the Earth-Moon system. This record is reduced or absent on Earth due to deflection of the solar wind and lower-energy cosmic rays by the geomagnetic field, and due to surface changes from active tectonism, associated volcanism, and surface weathering by atmospheric and hydrological processes.

Strategic Goal 6: Establish a lunar return program having the maximum possible utility for later missions to Mars and other destinations.

Mapping of chemical resources on the Moon from exogenic and internal sources prepares the way for human missions to the surface. Understanding effects of external space radiation on planetary surfaces and atmospheres paves the way for robotic and eventual human exploration of other planetary bodies. LunaSSOX is testbed mission for other destinations.

Related 2006 Heliophysics Roadmap Research Focus Areas

F. Open the Frontier to Space Environment Prediction - *Understand the fundamental physical processes of the space environment - from the Sun to Earth, to other planets, and beyond to the interstellar medium.*

F2. Understand the plasma processes that accelerate and transport particles.

F3. Understand role of plasma and neutral interactions in nonlinear coupling of solar system regions.

H. Understand the Nature of Our Home in Space - *Understand how human society, technological systems, and the habitability of planets are affected by solar variability interacting with planetary magnetic fields and atmospheres.*

H4. Apply our understanding of space plasma physics to the role of stellar activity and magnetic shielding in planetary system evolution and habitability.

J. Safeguard the Journey of Exploration - *Maximize the safety and productivity of human and robotic explorers by developing the capability to predict the extreme and dynamic conditions in space.*

J1. Characterize the variability, extremes, and boundary conditions of the space environments that will be encountered by human and robotic explorers.

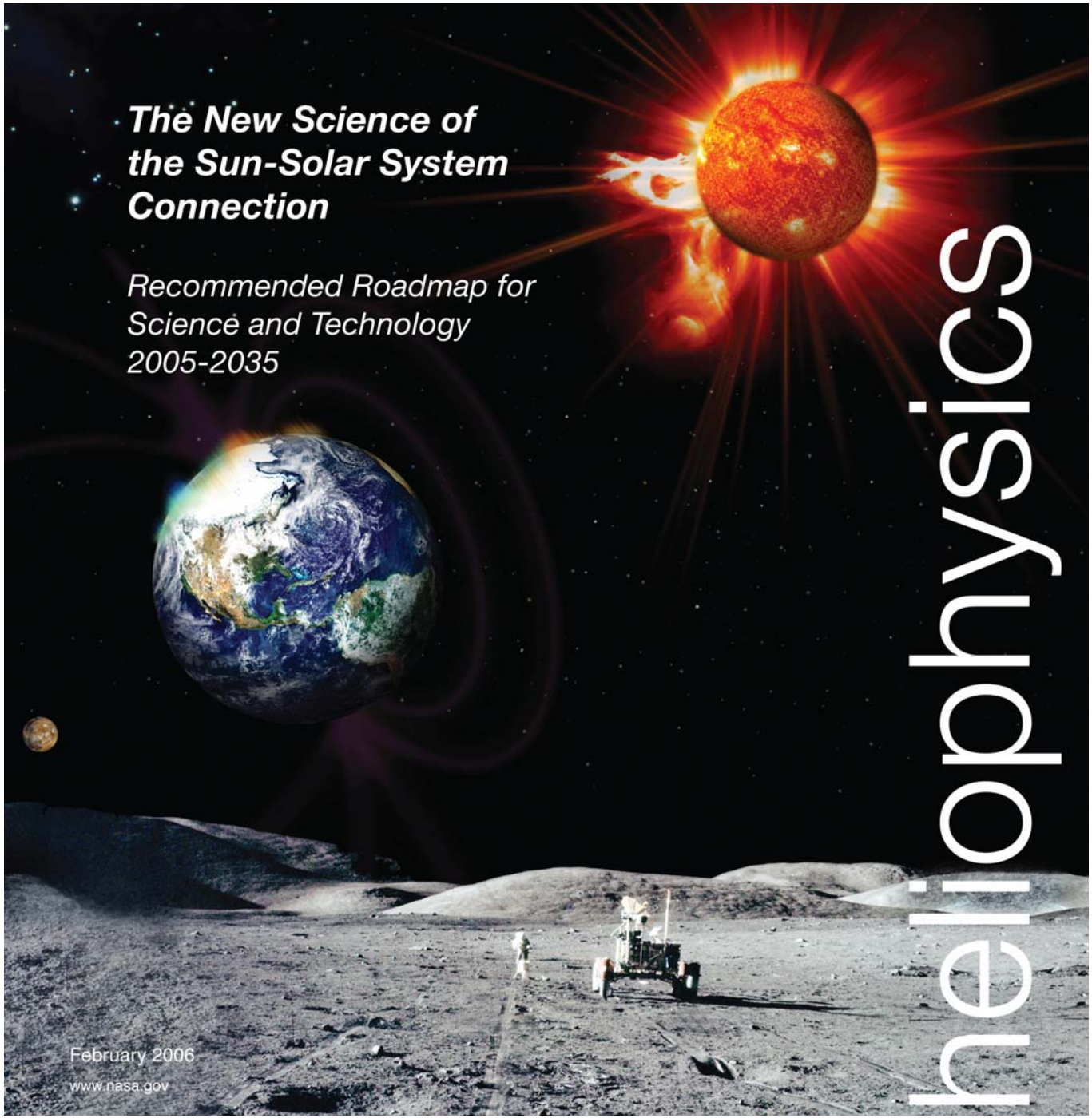
The New Science of the Sun-Solar System Connection
Recommended Roadmap for Science and Technology 2005-2035
heliophysics
February 2006
www.nasa.gov

Heliophysics Science and the Moon, *Report to NASA Advisory Council – Heliophysics Subcommittee, NP-2007-07-80-MSFC, Pub 8-40716, NASA MSFC, Sept. 2007.*

Relevant Objectives for LunaSSOX

- Characterize the Near-Lunar Electromagnetic and Plasma Environment
- Interaction of Plasma with the Moon
- Characterize and Understand the Interaction of Dust and Plasma on the Surface of the Moon and in the Lunar Exosphere
- Characterize Radiation Bombardment on the Lunar Surface and Subsurface
- History of the Sun and Cosmic Radiation
- History of the Inner Solar System According to the Lunar Cold Traps
- Analyze the Composition of the Solar Wind

And we also suggest:

Use the Moon as a heliophysics science platform to observe spatial and spectral structure of the solar corona and near-solar dust environment

Mission Implementation Description

***Location: LRO-type 50-km polar orbit after initial elliptical phase for lunar wake**

***Attitude control: 3-axis stabilized (ram, nadir, solar)**

Adjust to direction of solar wind, magnetosphere, & lunar neutral gas flows

Prograde and retrograde imaging of Sun at hourly lunar limb occultations

*** Instruments:**

Low-energy ion-neutral and energetic heavy ion mass spectrometers, magnetometer, electron reflectometer (20 kg/20 W)

UV-VIS-IR spectroscopic imagers - particular focus on near-IR for any lunar polar surface ice bands and for solar F-corona dust (30 kg/30 W)

Measurement Strategy:

- **Large scale lunar environment characterization in initial elliptical lunar orbit**
- **Primary near-lunar and remote surface measurements in circular polar orbit**
- **Hourly lunar limb occultations for solar F-corona, zodiacal light, and lunar atmospheric observations – doppler shift of solar Fraunhofer lines, dust absorption**

Enabling and Enhancing Technology Development:

- **High resolution plasma and neutral gas composition spectrometers integrated to energetic ion detectors for complete characterization of plasma/SEP interactions**
- **Compact steerable high-resolution UV-VIS-IR spectroscopic imaging system for solar F-Corona, lunar surface & atmosphere, and other geospace observations – not diffraction limited by onboard internal or external occulter !**
- **Lightweight solar-powered spacecraft bus system for flexible lunar orbital and solar observation operations**

THAR'S GOLD IN THAM LUNAR HILLS

Jan 28 2006 By Stephen White

Helium 3 could hold key to the future of space exploration. It could be the 'cash crop' for the Moon

RUSSIA is planning to beat America back to the Moon to mine for an abundance of untapped riches.

But it's not gold or diamonds they aim to bring back to Earth. … a total of 1,100,000 metric tons of He3 have been deposited by the solar wind on the Moon.

The total supply in the US strategic reserves is about 29 kg, and another 187 kg is mixed up with natural gas in storage.

Nikolai Sevastyanov, head of Russia's giant Energia Space Corporation, said: "We are planning to build a permanent base on the Moon by 2015 and by 2020 we can begin the industrial-scale delivery of helium 3."

… solar wind-implanted particles are more abundant on the far side, because the Earth (its magnetosphere) shields the Moon's near side from the solar wind for part of each solar orbit … the greatest amounts of helium 3 will be found on the far side of the Moon.

DailyRecord.co.uk

Solar Wind Irradiation Geometry for the Moon

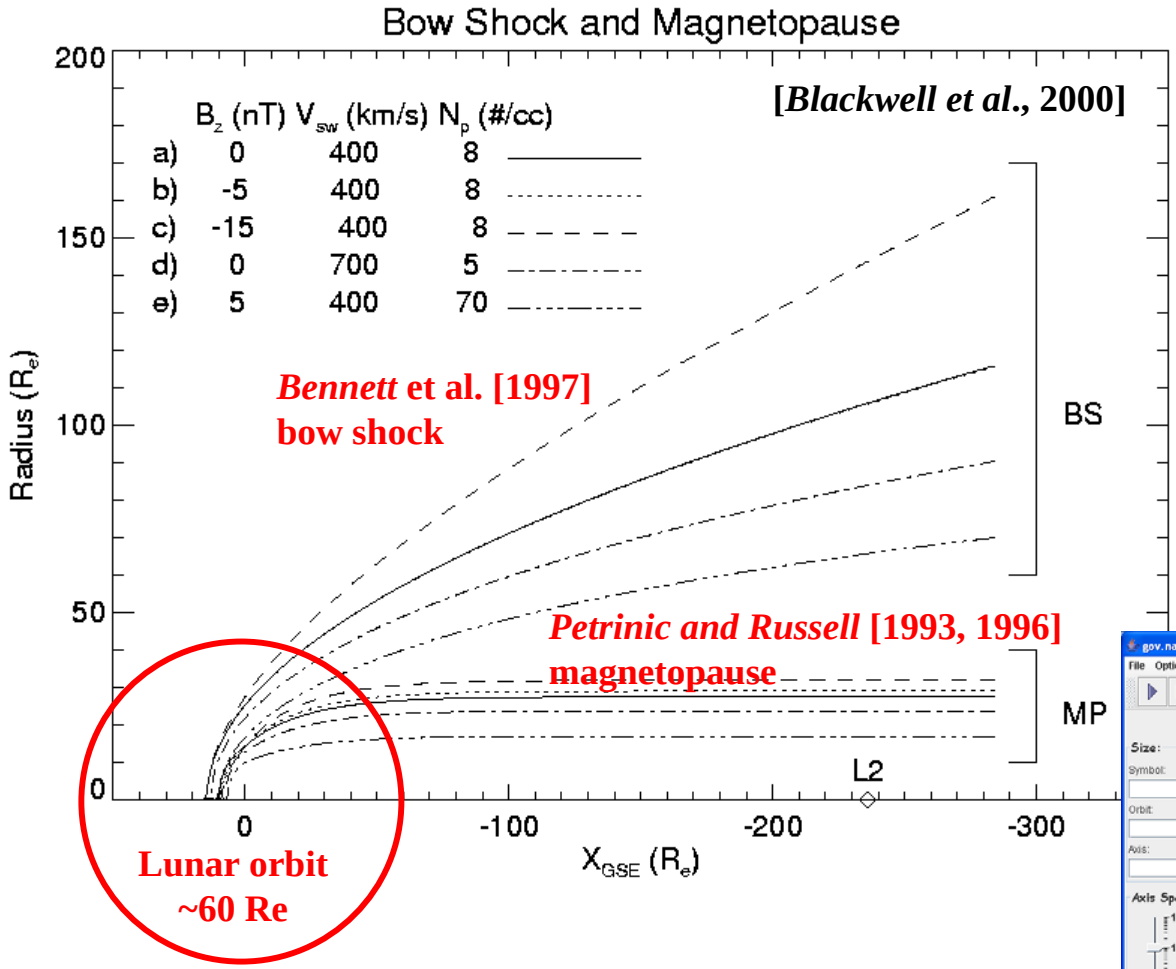

Subsolar proton irradiation of the lunar surface occurs preferentially on the farside which faces the Sun upstream of the terrestrial magnetosphere during the 28-day orbit

Graphics provided by J. Minow at Barrow 2008

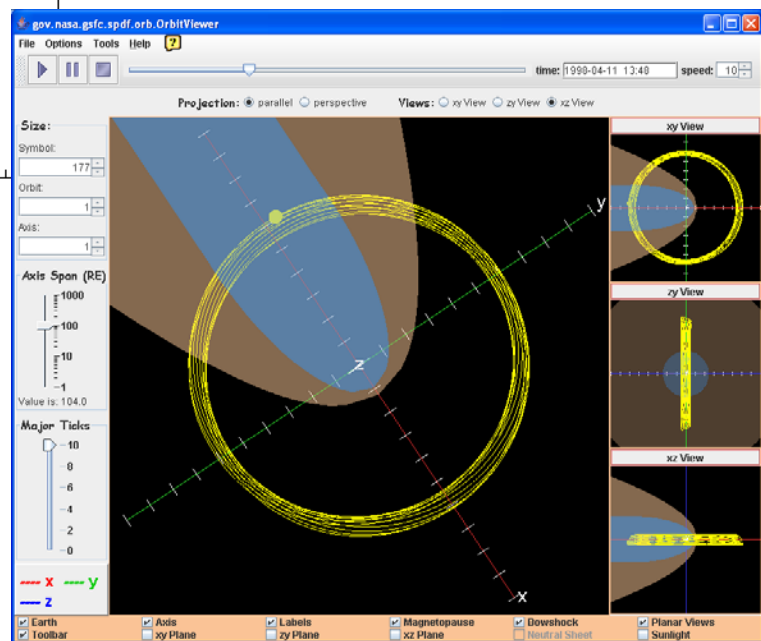

Fraction of Month in Plasma Environments

~73.5% solar wind	~20.6 days
~13.3% magnetosheath	~ 3.7
~13.2% magnetotail	~ 3.7

Lunar farside composition is intrinsically different from nearside composition and may differently affect adsorption and desorption of exogenic species from the solar wind and sputtering products of plasma-surface interactions elsewhere on the lunar surface

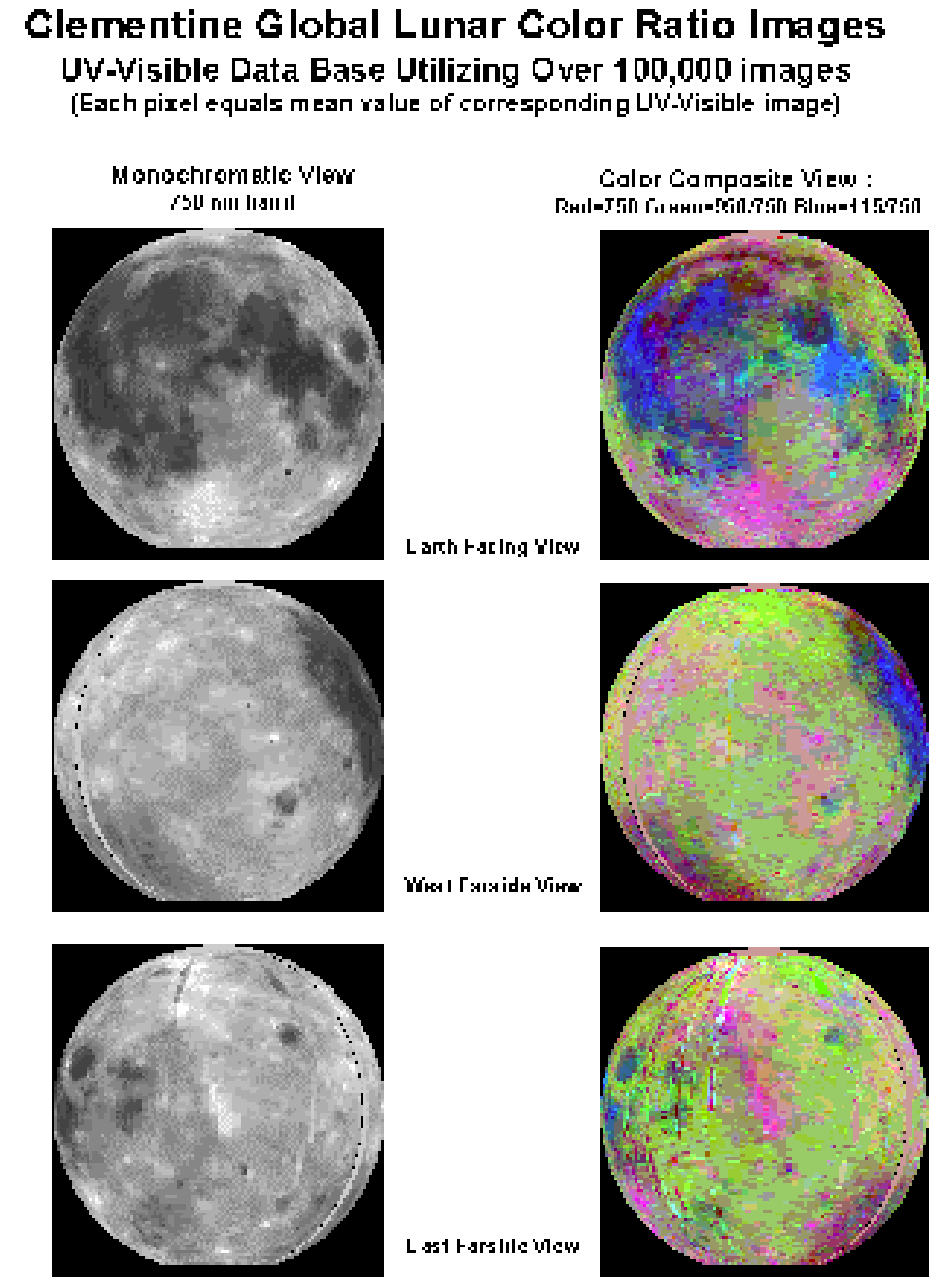

Near Side

Far Side

Far Side

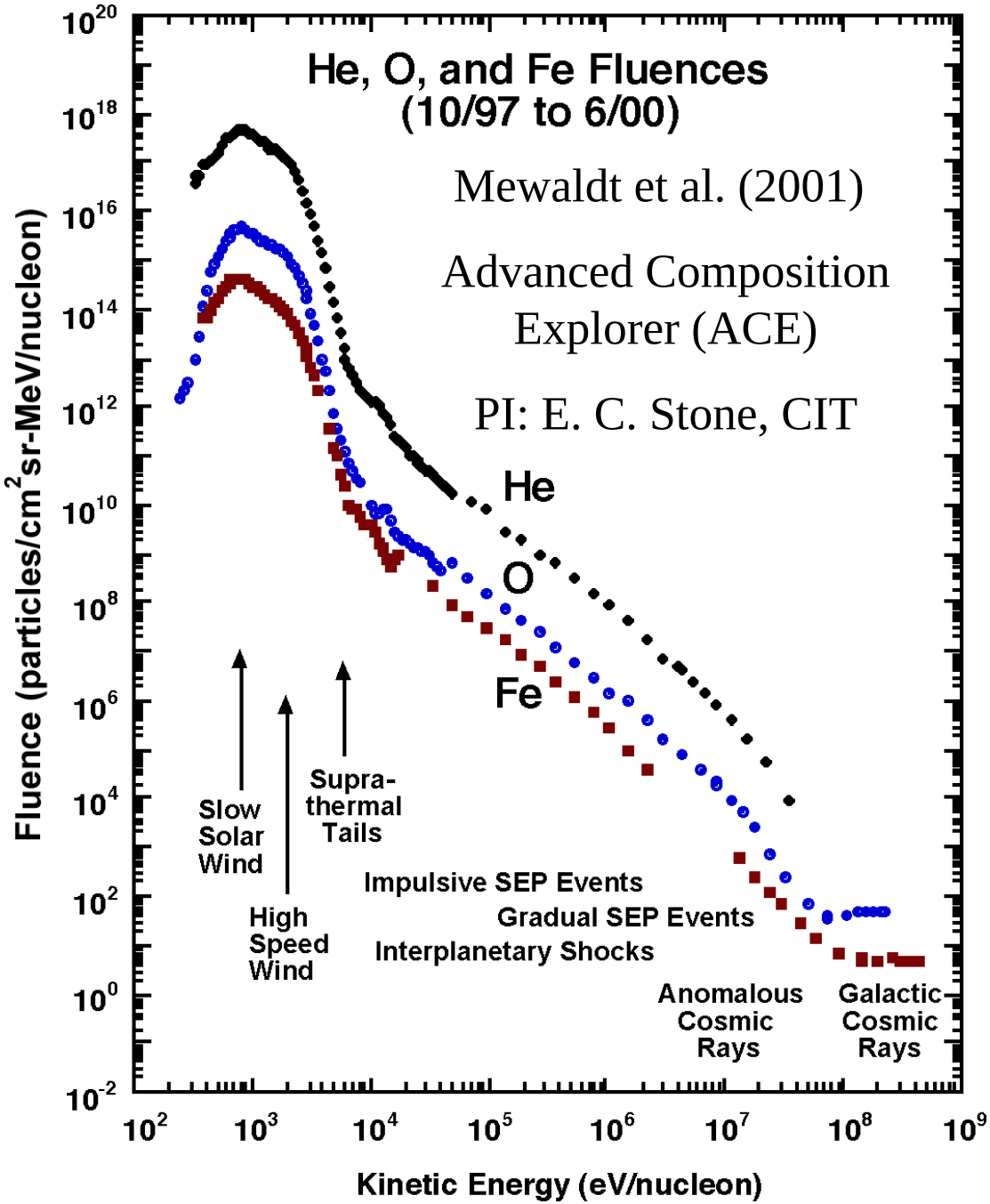

The full range of solar wind plasma to highly energetic ions from the Sun, and higher energy cosmic ray ions from the outer heliosphere and the galaxy, impacts the lunar surface as energy sources for sputtering, implantation (e.g., H, He^3, O), chemical radiolysis, and neutron production.

The ACE cumulative spectra (left) support modeling for long term effects of these processes at the lunar surface

Continuation of ACE and follow-on L1 missions is important to lunar interaction modeling and surface & atmospheric pickup ion measurements exploiting these interactions.

Lunar surface sputtering by solar wind & energetic ions generates a rich harvest of secondary ion species detectable from orbit

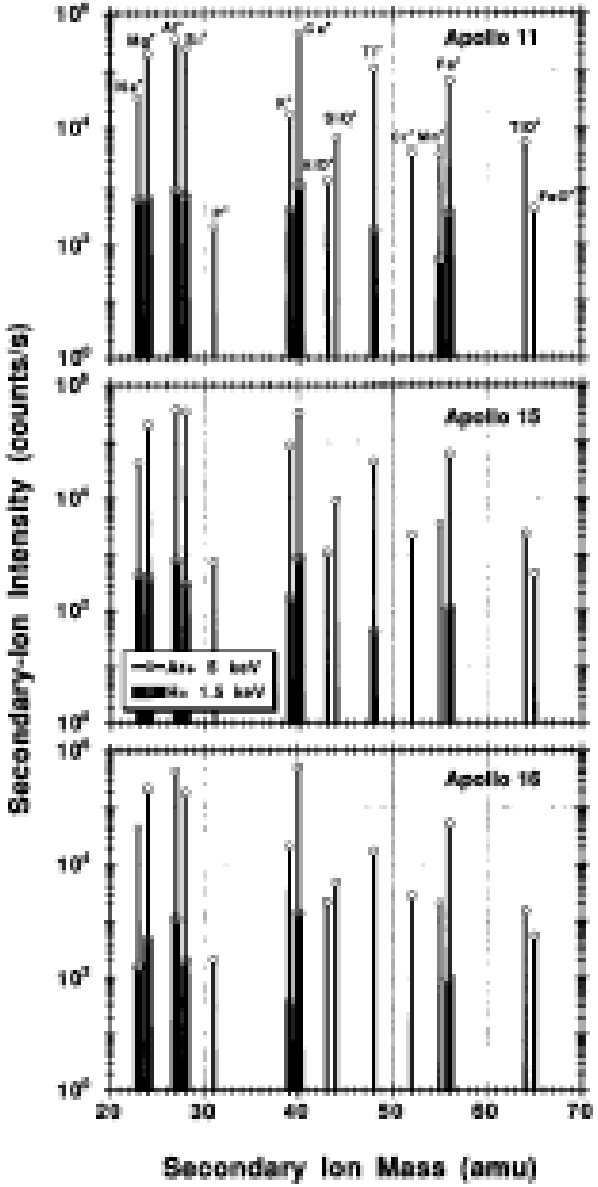

Fig. 1. Secondary-ion intensities of Na through FeO for incident ions of Ar at 5 keV, and solar wind-like ions of H at 1.5 keV, respectively. Secondary-ion intensities from the three lunar soil simulants are shown.

Elphic et al. [1991]

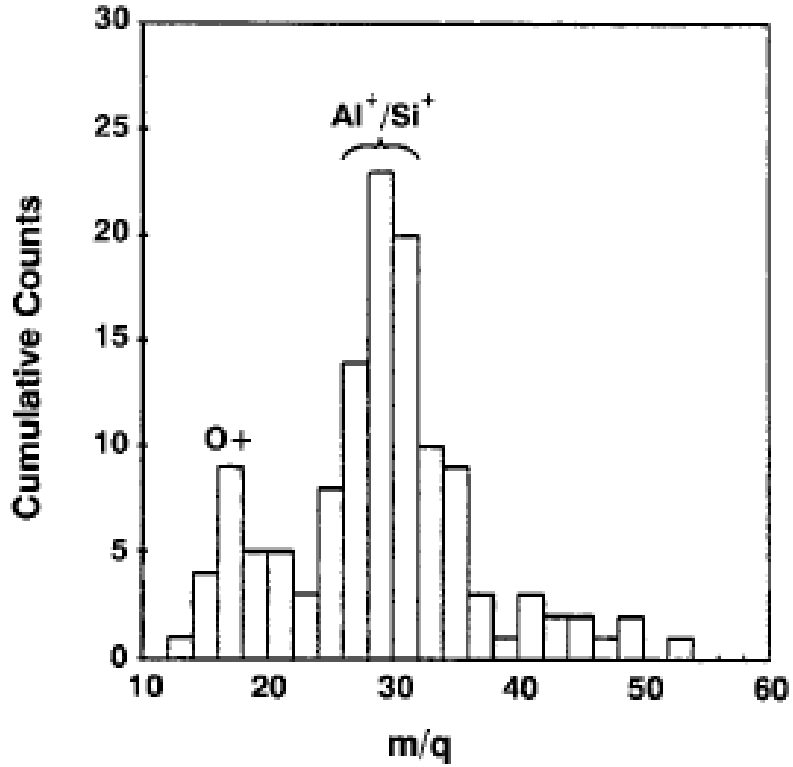

Figure 10. Mass-to-charge (m/q) spectra from the AMPTE/SULEICA instrument showing the detection of lunar ions when it was downstream of the Moon. Adapted from *Hilchenbach et al.* [1991].

From Stern [1999]
and Hilchenbach et al. [1991]

Atmospheric Species	Detectable Density /cc @ 1-Hz,1cm^2	Present Density Limits /cc [Stern 1999]
H	65	<17
He	336	2,000 (day)
C	164	<200
N	375	<600
O	321	<500
Na	17	70
S	167	<150
Ar	735	10^5 (day)
K	21	17
Xe	476	<3000
CH_4	11	10^4 (predawn)
N_2	140	800 (predawn)
CO	3.2	1,000 (predawn)
CO_2	115	1,000 (predawn)
H_2	7.6	<9,000
OH	6.3	$<10^6$

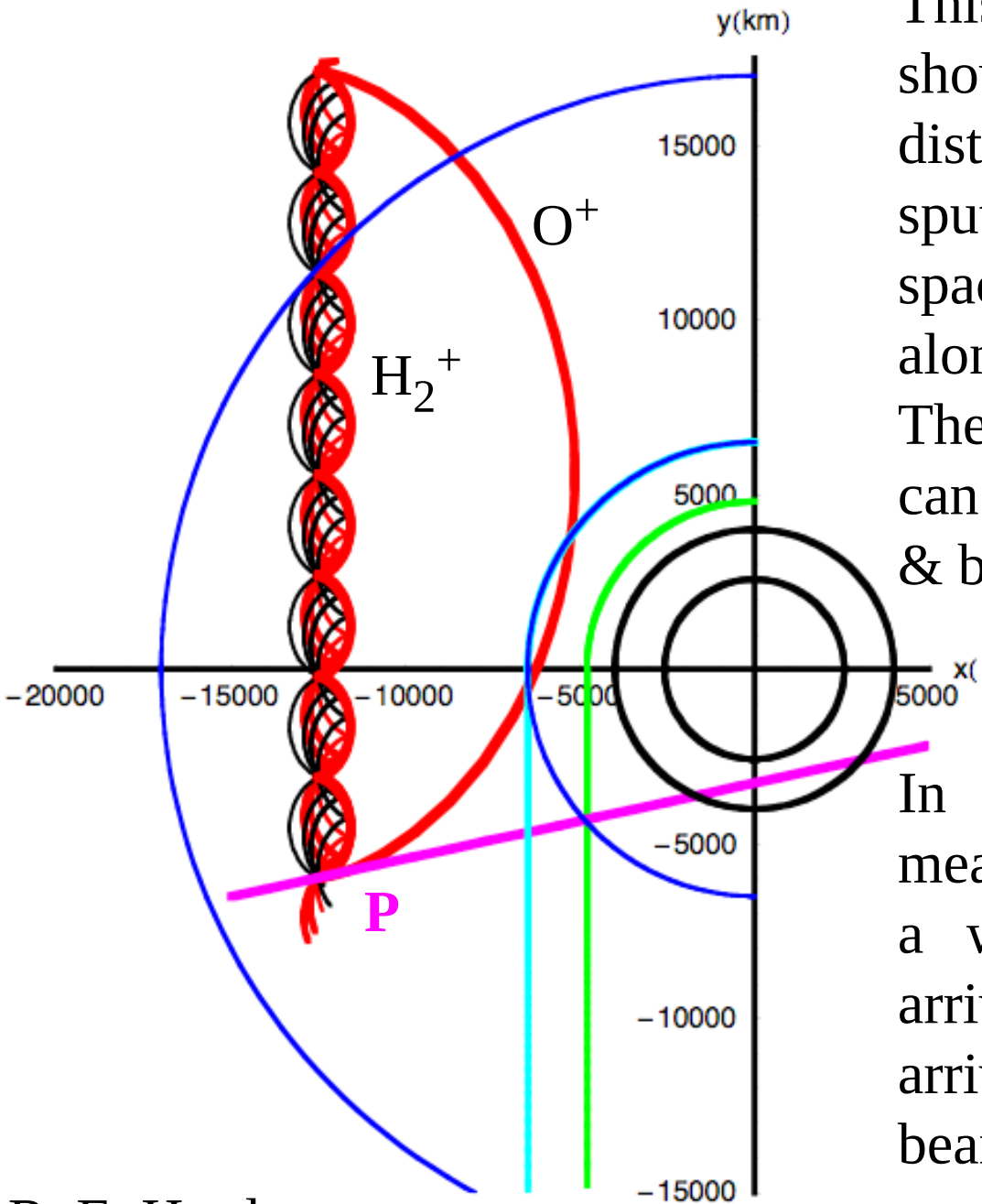

This moon-centric illustration shows the different directional distributions to be expected for sputtered ions measured by a spacecraft detector at point P along the pink trajectory line. The sample ions, H_2^+ and O^+, can originate from locii along red & black cycloidal origin curves.

In a 3-D plasma ion measurement the lighter ion has a widely distributed range of arrival directions but the O^+ ion arrives in a relatively narrow beam if the source is localized near or at the lunar surface.

R. E. Hartle

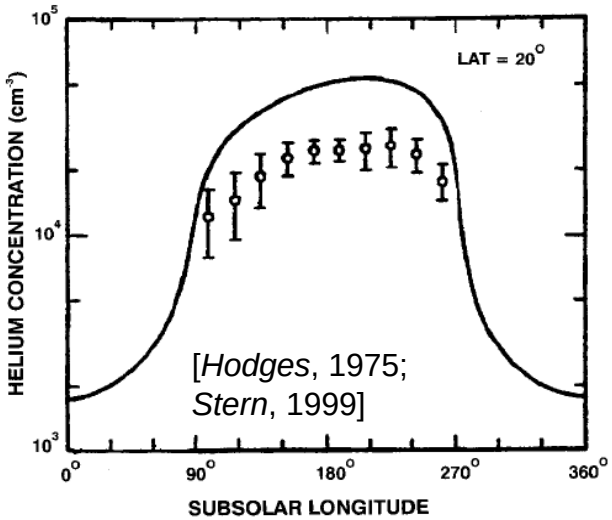

[*Hodges*, 1975; *Stern*, 1999]

Normalized He_4^+ ν flux, Φ_ν

(in flow direction)

Hartle and Sittler, 2007

$\mathrm{Log}_{10}\Phi_\nu$

−0.2
−0.4
−0.6
−0.8
−1.0

North Axis (E-Field) ψ

−2
−1
0
1
2

B-Vector Axis (IMF) ζ

−2
−1
0
1
2

Axial position units – lunar radii

Model computation of pickup He_4^+ density approximates subsolar local time distribution from Apollo

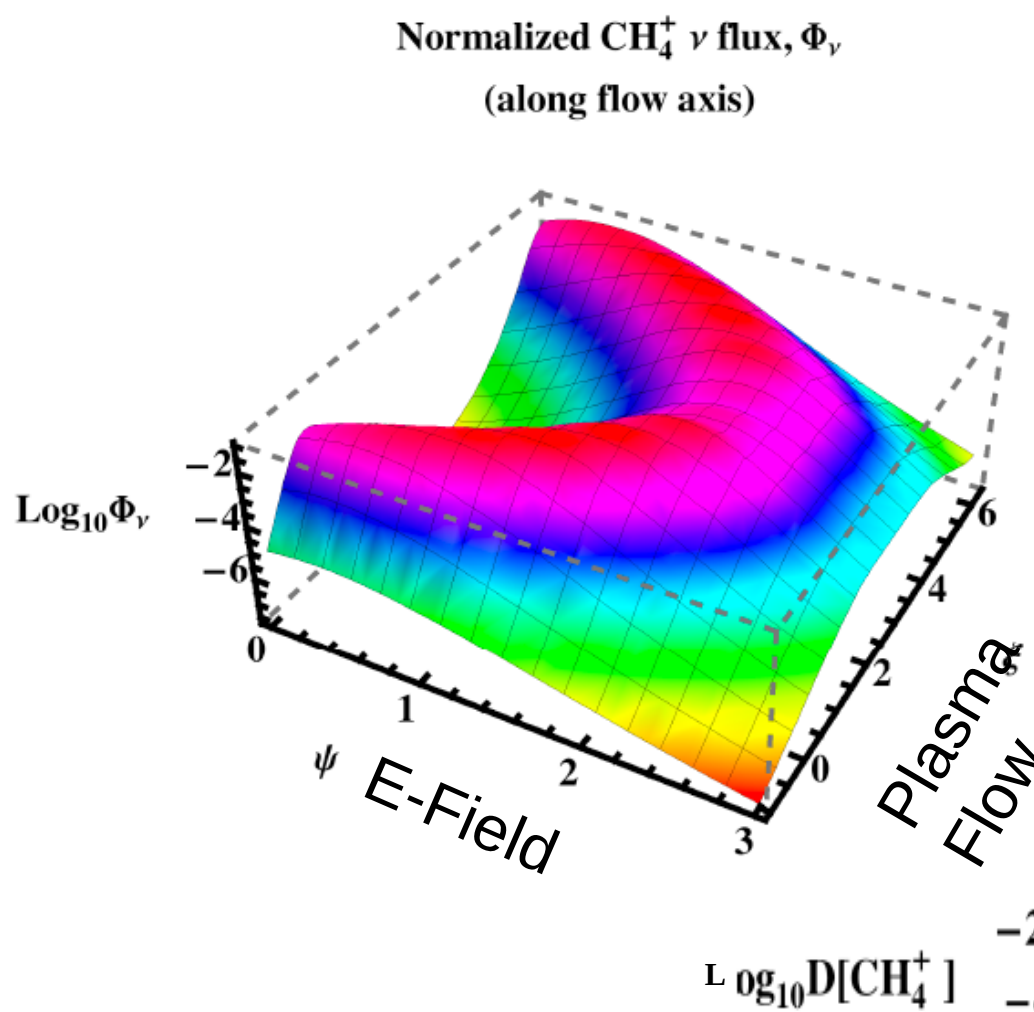

This Titan example under Moon-comparable conditions illustrates the geometry of downstream cycloidal motion for lunar CH_4^+ ions from the lunar surface to the wake region

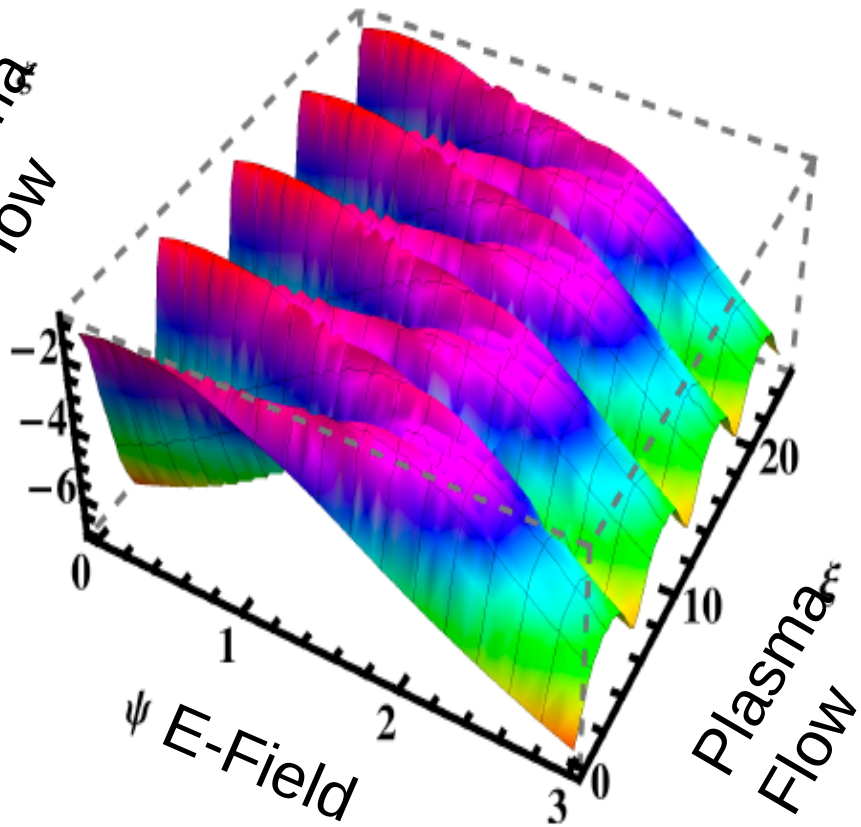

Axial position units – moon radii

Hartle et al., Fall AGU, 2007

Simulation of Magnetic Anomaly Interaction for SW H^+ and PUI O^+

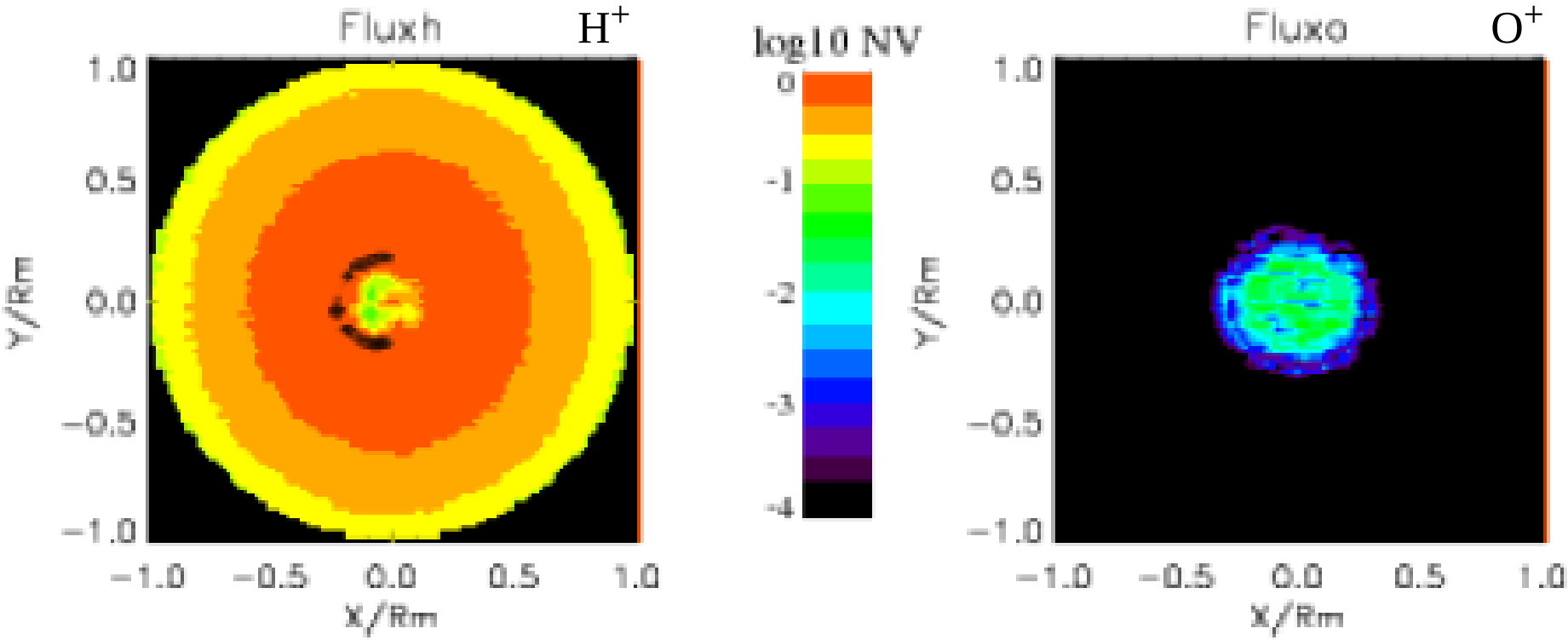

Dayside hemisphere distributions of surface fluxes for solar wind H^+ and atmospheric pickup O^+ ions incident on the Moon with simulated surface magnetic anomaly at the center. These X-Y views look in the +Z direction of bulk solar wind flow with the solar wind magnetic field in the +Y direction. The O^+ ions are swept by the solar wind into the moon in the central region around their points of origin, while H^+ ions impact the full sun-lit disk.

A. Lipatov (2007)

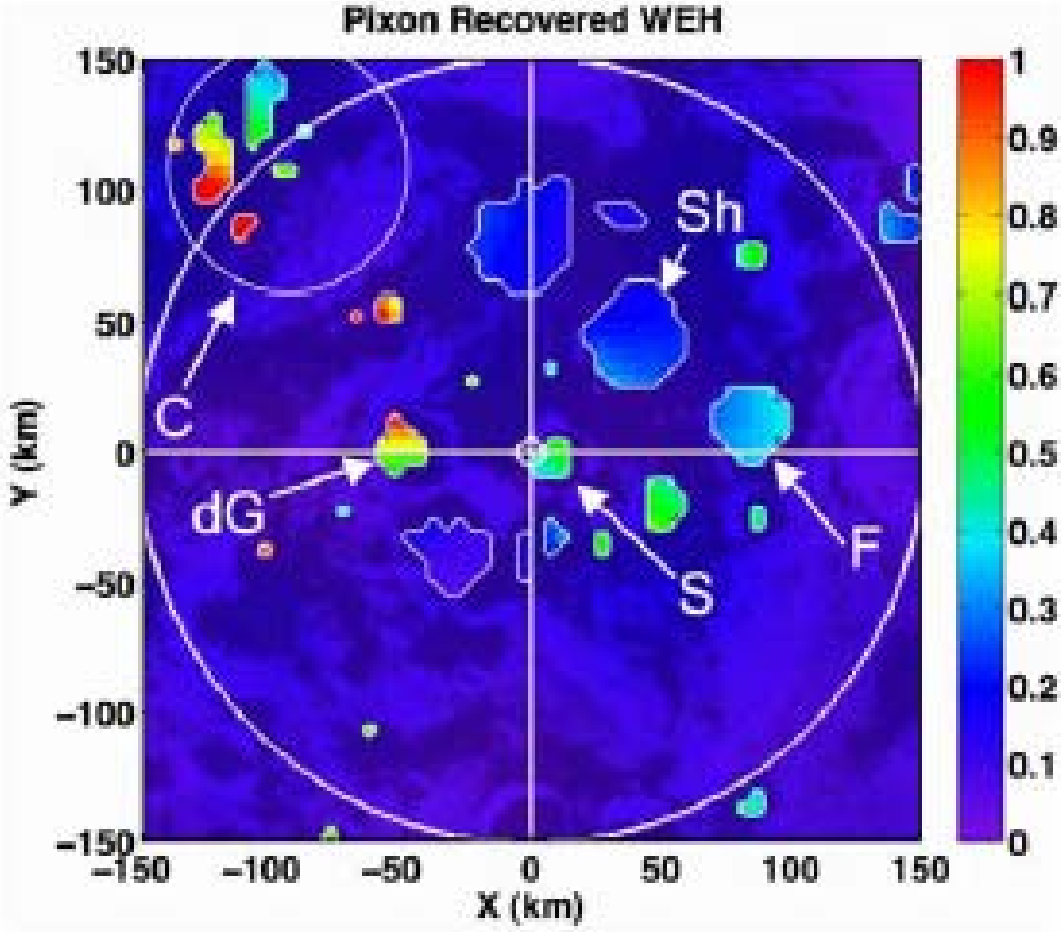

Energetic ions and Interstellar /Inner-Source pickup ions with large-scale cycloidal motions easily impact the shadowed polar craters and provide material for in-situ mass spectrometry at orbit of crater floor composition, potentially including water group species (OH) from ice mixed into the regolith.

Water-equivalent hydrogen (WEH) in wt% corresponding to the Lunar Prospector epithermal neutron count rates (Elphic et al., 2007). Large circle denotes 85°S, and Shackleton crater (S), site of NASA's planned polar lunar base, is located nearly at the south pole.

Simulated ion distributions at orbit scale with solar wind B & V

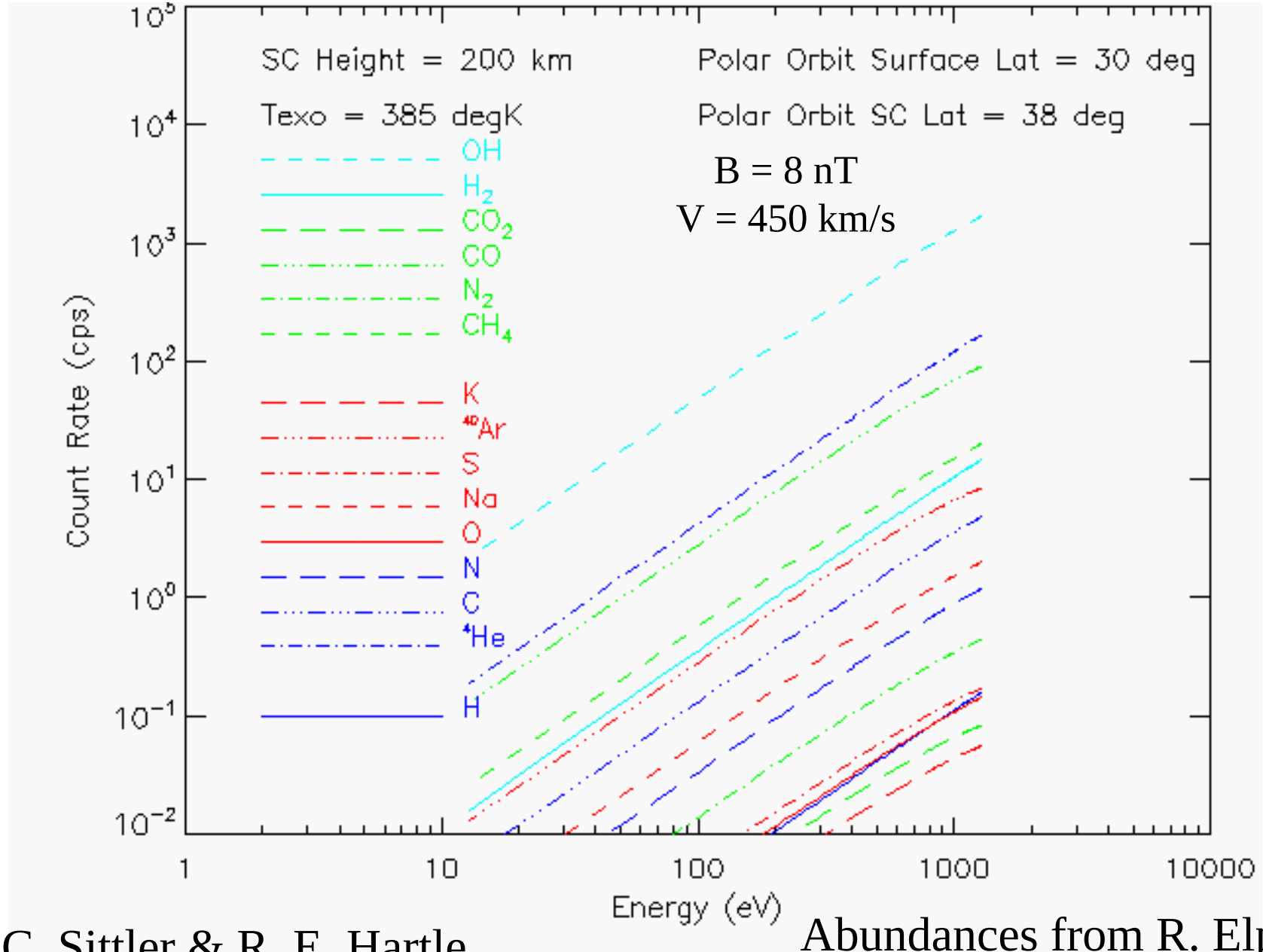

E. C. Sittler & R. E. Hartle

Abundances from R. Elphic

Sporadically Increasing B & V at Solar Max Increase PUI Fluxes

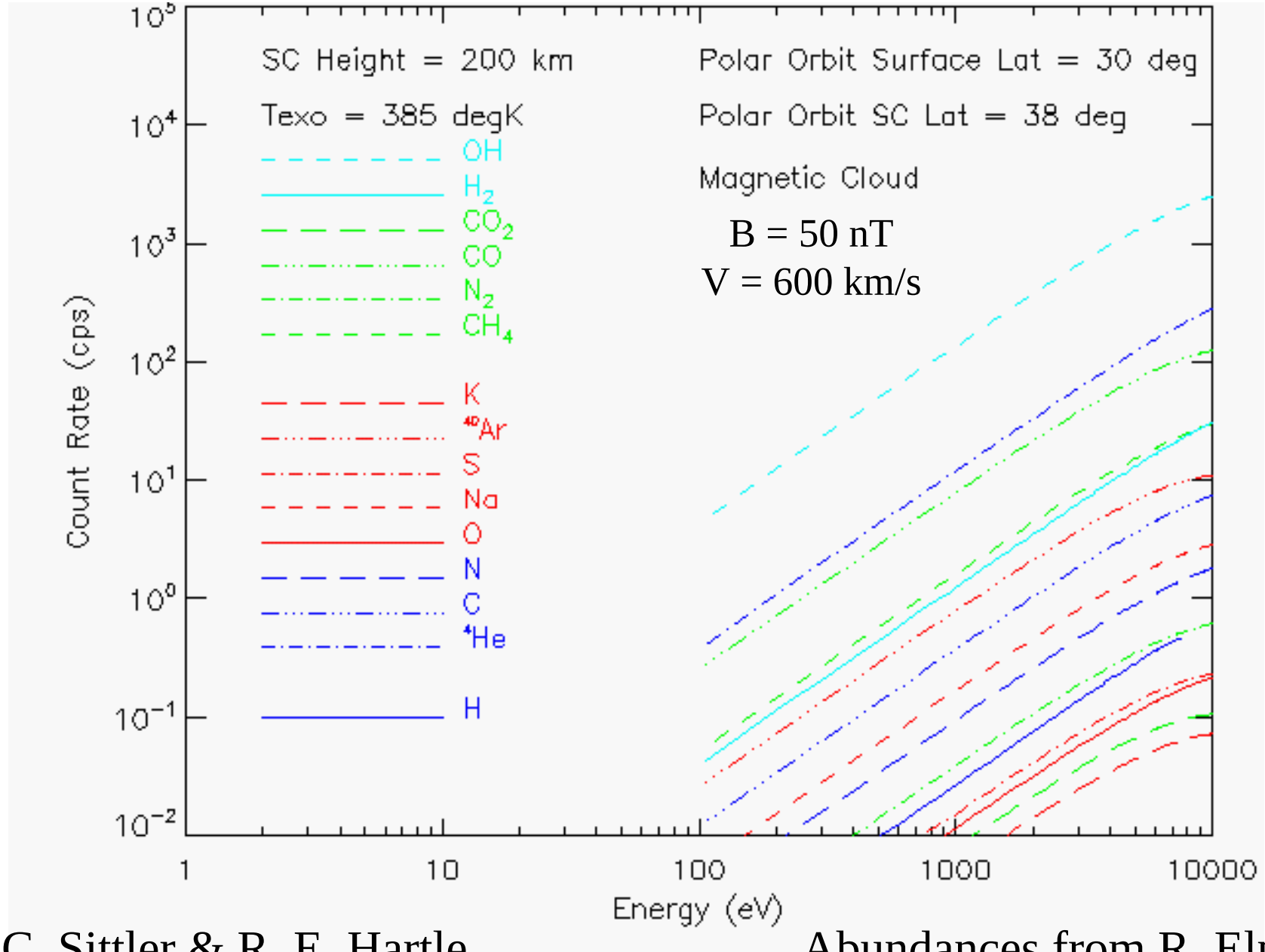

E. C. Sittler & R. E. Hartle

Abundances from R. Elphic

“Inner Source” of pickup ions from near-solar plasma-dust interactions near the Sun provides additional source of exogenic lunar composition

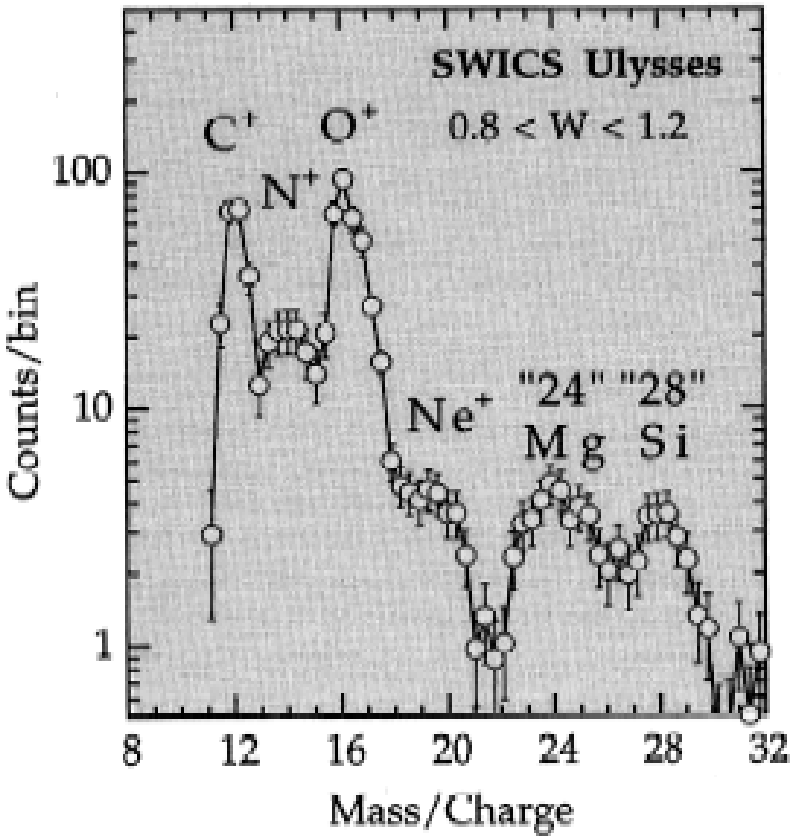

Figure 2. Mass per charge distributions of heavy pickup ions in the inner source. These data were taken over the same time period as in Figure 1. A five-point running average of counts in mass/charge bins > 17 was used to smooth the data. Peaks at mass/charge 24 and 28 are clearly visible, indicating the presence of singly charged Mg and Si (as well as C, N, O, and Ne) in the inner source.

From Gloeckler et al. (2000)

Table 1. Element Abundance Ratios (Relative to Ne) of the Inner Source Pickup Ions, the Low Solar Wind, and Energetic Particles Accelerated in CIRs

Element	Inner Source[a]	Solar Wind[b]	CIR Particles[c]
H	7710±1360[d]	12000±5100	33100±10500
He	---------	900±260	1000±88
C	4.57±0.38	8.1±1.1	4.88±0.25
N	1.24±0.16	1.5±0.2	0.91±0.12
O	3.13±0.18	11.4±0.9	6.25±0.31
Ne	1.00±0.17	1.00±0.10	1.00±0.13
Mg	1.52±0.19	1.40±0.28	0.70±0.09
Si	0.99±0.18	1.30±0.17	0.70±0.19

[a]Pickup ions from the low and middle latitude (< 60°) extended inner source (present work).

[b]Average of the fast and slow solar wind abundances compiled by *von Steiger et al.* [1997]. The solar wind Ne abundance we derived from SWICS data using a sophisticated composition analysis developed by N. A. Schwadron et al. (Techniques for analysis of data from time-of-flight instruments, submitted to *Journal of Geophysical Research*, 1999b).

[c]Compiled by *Keppler* [1998].

[d]Errors are due to statistical uncertainties only.

Inner Source has solar wind abundance for Ne-Si but is underabundant for H-O: dust-plasma interaction effect?

Primary dust-plasma interaction zone in the solar F-corona is visible to multi-wavelength observations under otherwise-rare total eclipse conditions approximated by hourly lunar limb occultations of the solar disk during the envisaged LunaSSOX mission. This zone may begin at 3-4 solar radii inner boundary dependent on composition of the grains which destructively sublimate on approaching this boundary during inward motion. High-resolution Fraunhofer line spectroscopy with doppler filters could resolve high-speed keplerian motions of the grains against lunar & zodiacal dust foreground.

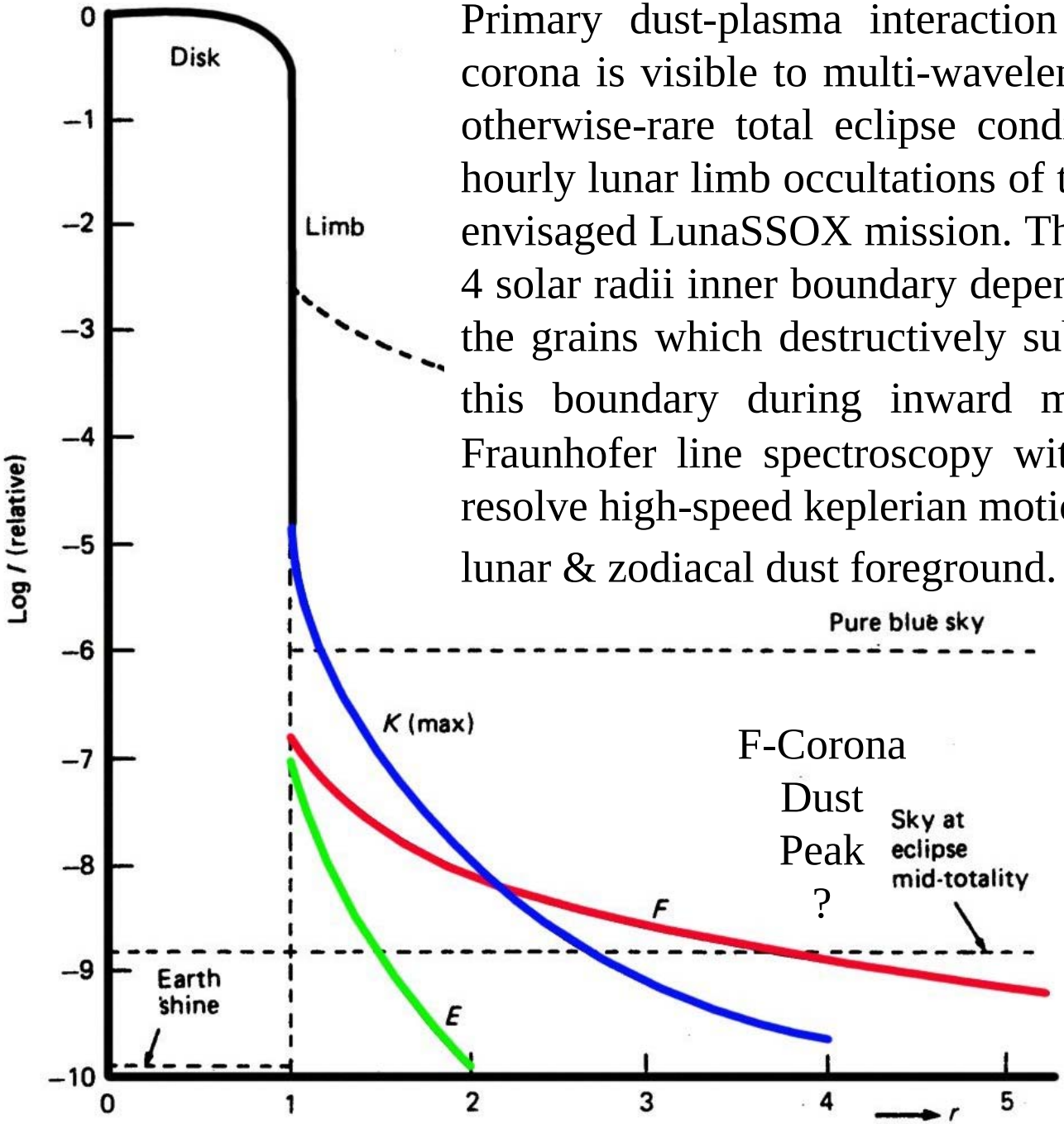

Apparent dust peaks at 4 R_{sun} were seen at some wavelengths (e.g., near IR) in 1966-67 to 1983 but not thereafter (Mann et al., 2004) – solar cycle effects?

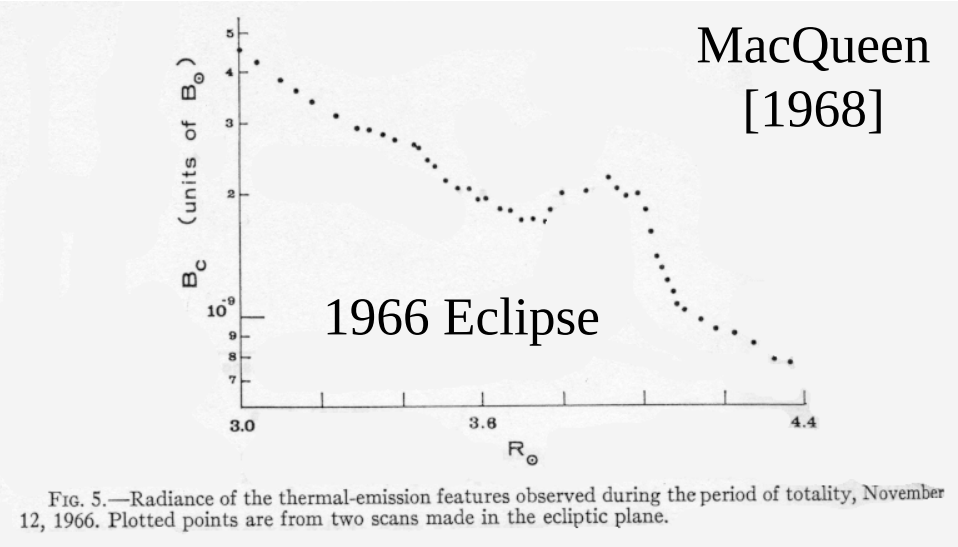

FIG. 5.—Radiance of the thermal-emission features observed during the period of totality, November 12, 1966. Plotted points are from two scans made in the ecliptic plane.

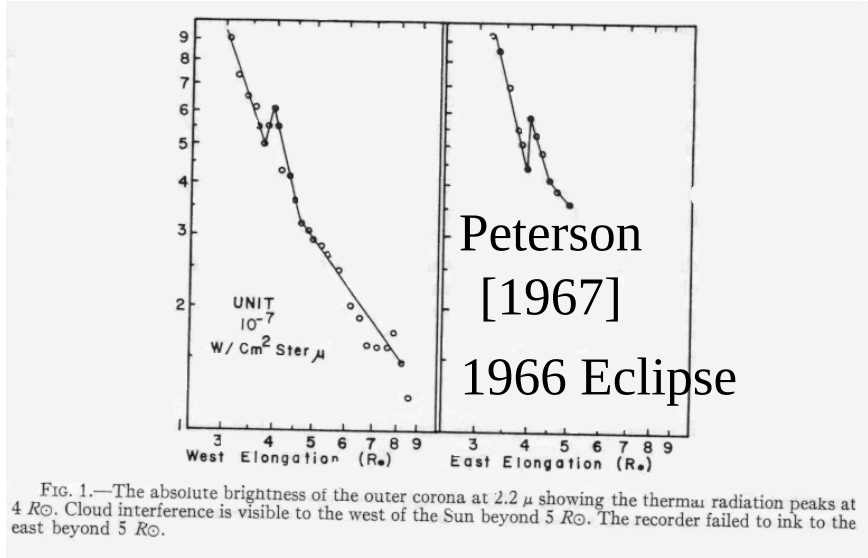

FIG. 1.—The absolute brightness of the outer corona at 2.2 μ showing the thermal radiation peaks at 4 $R_\odot$. Cloud interference is visible to the west of the Sun beyond 5 $R_\odot$. The recorder failed to ink to the east beyond 5 $R_\odot$.

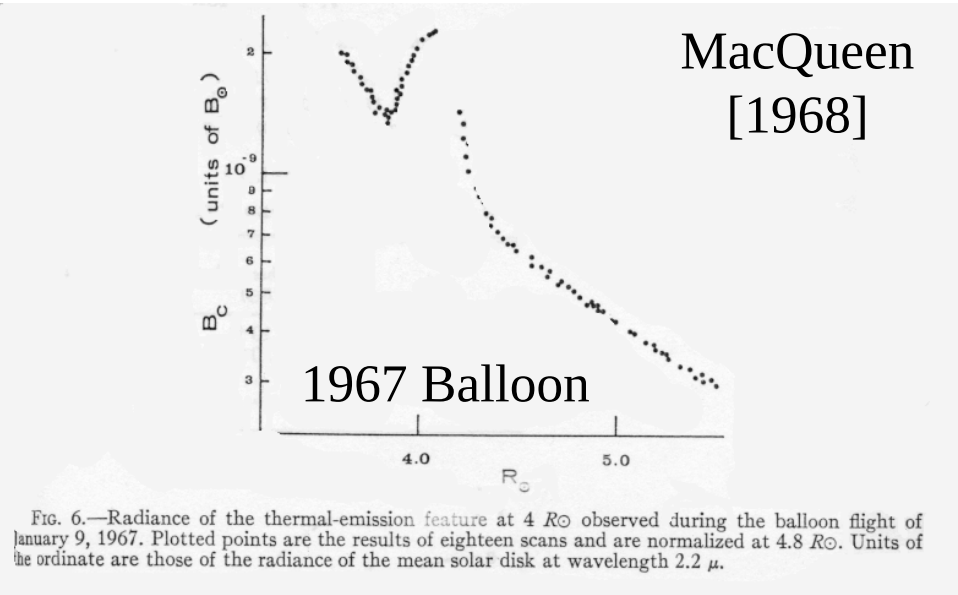

FIG. 6.—Radiance of the thermal-emission feature at 4 $R_\odot$ observed during the balloon flight of January 9, 1967. Plotted points are the results of eighteen scans and are normalized at 4.8 $R_\odot$. Units of the ordinate are those of the radiance of the mean solar disk at wavelength 2.2 μ.

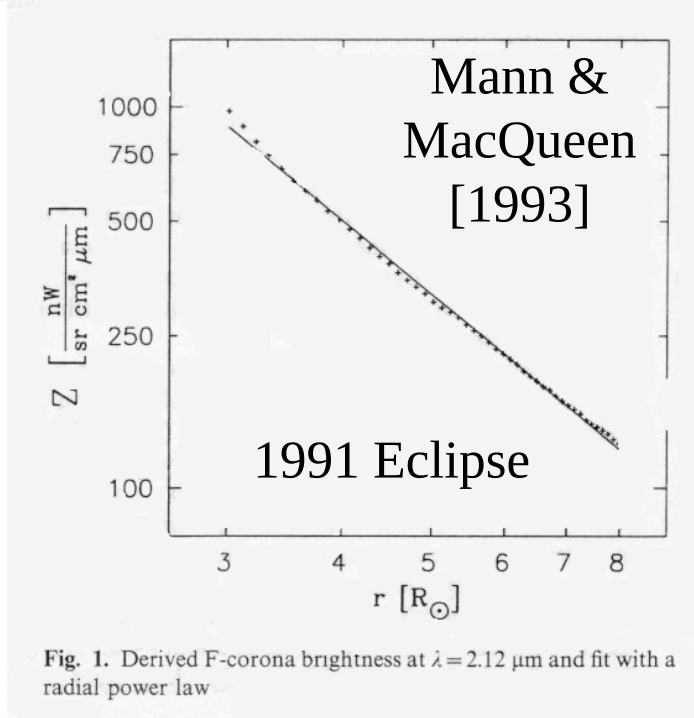

Fig. 1. Derived F-corona brightness at $\lambda = 2.12$ μm and fit with a radial power law

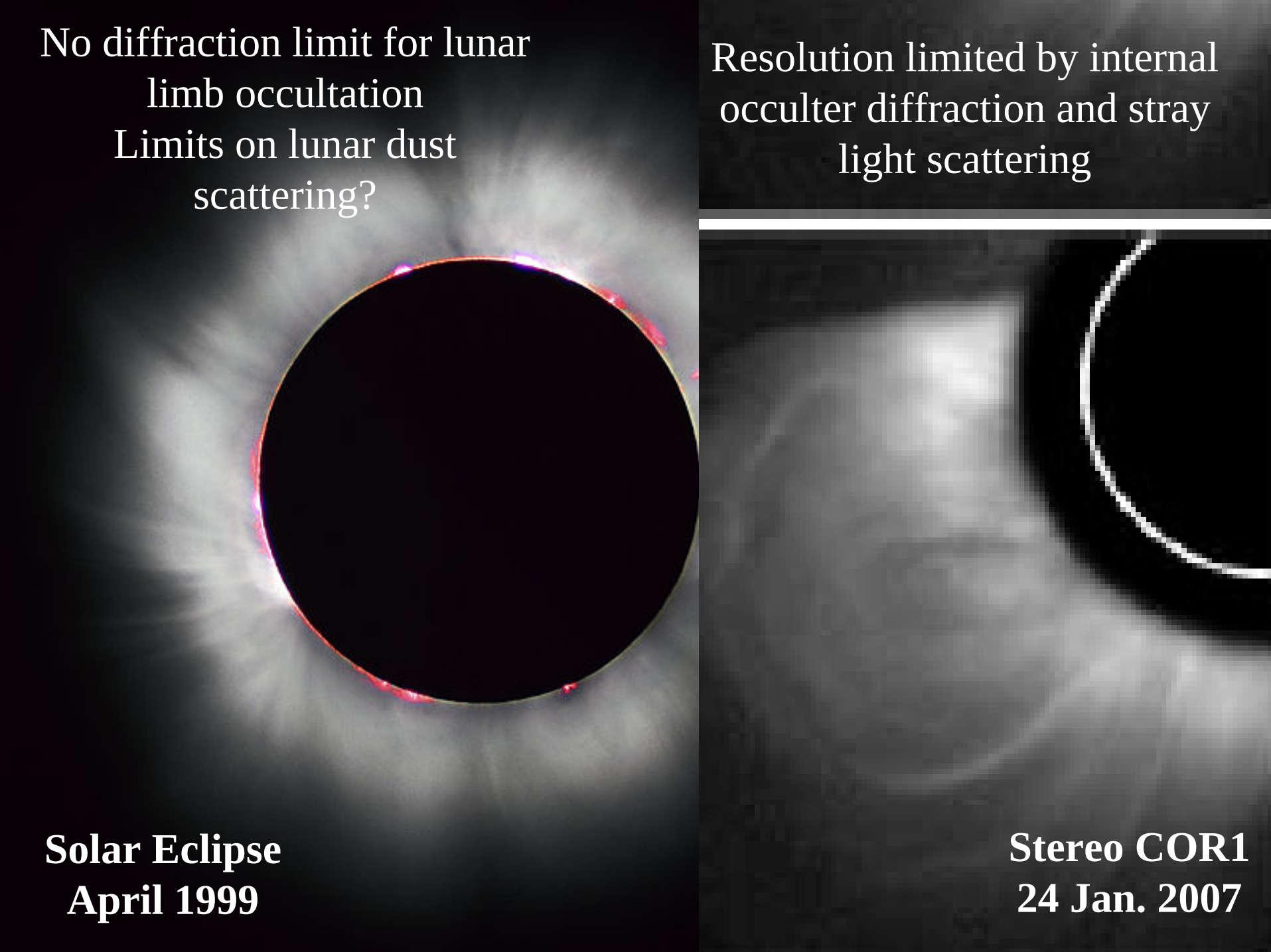
No diffraction limit for lunar limb occultation
Limits on lunar dust scattering?
Resolution limited by internal occulter diffraction and stray light scattering
Solar Eclipse
April 1999
Stereo COR1
24 Jan. 2007

Kaguya Earthrise observations demonstrate high-definition limb occultation effect that could be utilized by LunaSSOX orbiter

Conclusions

- Solar wind interaction imparts exogenic source of volatile and some refractory mass flow from Sun to Moon surface
- Direct primary plasma & SEP ion measurements, coupled to those of sputtered pickup ions, support global mapping of exogenic and endogenic components of lunar surface composition
- LunaSSOX hourly lunar limb occultation of solar disk from LRO-type orbit would allow frequent periodic measurements of near-solar plasma-dust dynamics and composition in the “Inner Source” region contributing pickup ions to solar wind bombardment of the lunar surface. Lunar dust foreground effect needs more study.
- The Moon can be an integral part of the Heliophysics Global Observatory for solar and geospace observations

References

Elphic, R. C., et al., Lunar surface composition and solar wind-induced secondary ion mass spectrometry, Geophys. Res. Lett, **18**, 2165-2168, 1991.

Elphic, R. C., et al., Models of the distribution and abundance of hydrogen at the lunar south pole, Geophys. Res. Lett., **34**, L13204, DOI:10.1029/2007GL029954, 2007.

Gloeckler, G., et al., Elemental composition of the inner source pickup ions, J. Geophys. Res., **105(A4)**, 7459, 2000.

Hartle, R. E., and R. Killen, Measuring Pickup Ions to Characterize the Surfaces and Exospheres of Planetary Bodies: Applications to the Moon, *Geophys. Res. Lett.*, **33**, L05201, doi:10.1029/2005GL024520, 2006.

Hartle, R. E., and E. C. Sittler, Pickup ion phase space distributions: Effects of atmospheric spatial gradients, Journal of Geophysical Research (Space Physics) **112**, A07104, 2007.

Hilchenbach, M., et al., Detection of singly ionized energetic lunar pick-up ions upstream of Earth's bow shock, in *Solar Wind Seven*, edited by E. Marsch and G. Schwenn, pp. 150–155, Pergamon, New York, 1991.

Johnson, R.E. and E.C. Sittler Jr., Sputter-produced plasma as a measure of satellite surface composition: The Cassini Mission, *Geophys. Res. Lett.*, **17**, 1629, 1990.

MacQueen, R. M., Infrared observations of the outer solar corona, Astrophys. J., **154**, 1059-1076, 1968.

Mann, I., et al., Dust near the Sun, Sp. Sci. Rev., **110**, 269-305, 2004.

Mann, I., and R. M. MacQueen, The solar F-corona at 2.12 micron: calculations of near-solar dust in comparison to 1991 eclipse observations, Astron. Astrophys., **275**, 293-297, 1993.

Mewaldt, R. A., et al., Long term fluences of energetic particles in the heliosphere, in *Solar and Galactic Composition, AIP Conf. Proc. 598*, pp. 165-170, R. F. Wimmer-Schweingruber (ed.), AIP, Melville, NY, 2001.

Peterson, A. W., Experimental detection of thermal radiation from interplanetary dust, Astrophys. J., **148**, L37-L39, 1967.

Stern, S. A., The lunar atmosphere: history, status, current problems, and context., Rev. Geophys., **37**, 453-491, 1999.